

1  
2  
3  
4  
5 **Title**

6 Temperate-tropical transitions are linked with shifts in the structure of evolutionary integration in  
7 Vitaceae leaves

8 **Authors**

9 C. Tomomi Parins-Fukuchi<sup>1\*</sup>, Gregory W. Stull<sup>2,3</sup>, Jun Wen<sup>2</sup>, Jeremy M. Beaulieu<sup>4</sup>

10 **Affiliations**

11 <sup>1</sup>Department of Ecology and Evolutionary Biology, University of Toronto, Toronto, Ontario, Canada  
12 M5S 3B2.

13 <sup>2</sup>Department of Botany, National Museum of Natural History, Smithsonian Institution, Washington,  
14 DC 20013, USA.

15 <sup>3</sup>Germplasm Bank of Wild Species, Kunming Institute of Botany, Chinese Academy of Sciences,  
16 Kunming 650201, China.

17 <sup>4</sup>Department of Biological Sciences, University of Arkansas, Fayetteville, Arkansas, USA.

18 \*Corresponding author; email: tomo.fukuchi@utoronto.ca  
19  
20  
21  
22

23 **Abstract**

24 Understanding how the intrinsic ability of populations and species to meet shifting selective demands  
25 shapes evolutionary patterns over both short and long timescales is a major question in biology. One  
26 major axis of evolutionary flexibility can be measured by phenotypic integration and modularity. The  
27 strength, scale, and structure of integration may constrain or catalyze evolution in the face of new  
28 selective pressures. We analyze a dataset of seven leaf measurements across Vitaceae to examine  
29 whether the structure of macroevolutionary integration is linked to transitions between temperate and  
30 tropical habitats by examining how the structure of integration shifts at discrete points along a  
31 phylogeny. We also examine these patterns in light of lineage diversification rates to understand how  
32 and whether patterns in the evolvability of complex multivariate phenotypes are linked to higher-level  
33 macroevolutionary dynamics. We found that shifts in the structure of macroevolutionary integration in  
34 leaves coincide with early colonization events into new climates and that lineages that are more  
35 climatically labile are more weakly integrated overall. These more evolutionarily flexible lineages also  
36 had higher lineage turnover, suggesting a link between shifting vectors of selection, internal constraint,  
37 and lineage persistence in the face of changing environments.  
38

39 **Introduction**

40 Phenotypic traits often covary. The causes, consequences, and biological significance of trait  
41 covariation are complex and manifest distinct patterns across levels of temporal and biological scale.  
42 Trait covariation provides a numeric basis for partitioning the phenotype into semi-autonomous  
43 regions, where suites of traits internally covary, but are independent from one another. This is referred  
44 to as modularity (Wagner et al., 2007). The evolution of modularity and its relationship to major  
45 unanswered questions in evolutionary theory has long been intuited, but few empirical links have been  
46 drawn between the modular patterns that emerge at different levels of the biological hierarchy.  
47 Examples at a handful of these levels follow.  
48

49 Trait covariation has long been used to characterize internal constraints on adaptation within  
50 populations of organisms (e.g., Cheverud 1984, 1988; Wagner and Altenberg 1996). At this level, trait  
51 covariation is typically thought to reflect the genetic variance/covariance (VCV) matrix, i.e., the  
52 additive genetic variance shared between each trait pair (Cheverud 1988). The biological significance  
53 of this is straightforward. Trait pairs that share a lot of underlying genetic architecture will be  
54 constrained in their evolution by the functional demands of each other. The consequences of  
55 covariation on adaptation have been fruitfully explored in *Drosophila*. For example, Chenoweth and  
56 colleagues (2010) found that divergence between nine *Drosophila* populations aligned more closely  
57 with the orientation of the VCV than with the direction of experimentally induced sexual selection. In  
58 another case study, Hansen and colleagues (2003) found that the direction and strength of floral  
59 evolution over the short term was strongly predicted by constraints induced by covariation. Numerous  
60 similar examples exist (Bolstad et al. 2014, Sztepanacz and Houle 2019). However, results are mixed,  
61 with many studies suggesting that directional selection can overcome variational constraints (Beldade  
62 et al. 2002, Agrawal and Stinchcombe 2009). Computer simulations have even shown that directional  
63 selection itself may lead to the breakup and rearrangement of patterns in covariation (Melo and  
64 Marroig 2015). And so, selection-induced shifts in the structure of modularity might help facilitate the  
65 emergence of new, perhaps complex, adaptations. It appears sensible, then, to conceive of  
66 ‘evolvability’ – the ability for a population to respond to selection – as an axis that varies as a function  
67 of how well constraints are aligned with selection vectors and the capability for covariation patterns  
68 themselves to shift (Houle 1992, Hansen and Houle 2008).

69

70 Expanding temporal scale outward, the evolution of covariation patterns has repeatedly come up in  
71 paleontological and macroevolutionary studies. In these studies, covariation is measured using a  
72 diversity of approaches and data sources and so may perhaps be best considered more broadly as  
73 reflecting the general structure of modularity that emerges over long evolutionary timescales. It is  
74 possible that the origin of new morphologies is facilitated by shifts in the structure of modularity.  
75 Qualitative morphological analysis (Vermeij 1973), shifts in patterns displayed by discrete traits  
76 (Wagner 2018), and coordinated patterns in evolutionary disparity and rate among suites of quantitative  
77 traits (Parins-Fukuchi 2020) have all been used to reach this conclusion. Paleontological work also  
78 suggests that shifts in the strength of covariation may mediate long-term trends in phenotypic evolution  
79 (Goswami et al. 2015). A parallel but distinct avenue of research has also shown that changes in the  
80 strength of correlation between pairs of traits may underlie ecological transitions (Revell and Collar  
81 2009, Revell et al. 2022). All of these diverse contexts are consistent with the population genetic notion  
82 that phenotypic innovations may correspond to changes in ‘parcellation’ and ‘integration’ (i.e.,  
83 separating and joining together, respectively) of traits (Wagner and Altenberg 1996), but no explicit  
84 links have been drawn. The impact of constraint induced by integration patterns on macroevolutionary  
85 patterns, such as lineage survival, are also very poorly known.

86

87 Trait covariation has also been explored in the context of ecological community assembly. When  
88 measured within plant communities, each aligned along an environmental gradient, trait covariation  
89 varies as a function of environmental stress (Dwyer and Laughlin 2017, Brown et al. 2022). This  
90 pattern probably results from the functional inviability of some trait combinations within certain  
91 climates. In this scenario, lineages with unfavorable trait combinations or covariation patterns are  
92 filtered out of some regions. While useful from the standpoint of functional ecology, these studies do  
93 not tell us how variation in covariation patterns itself arises, nor how or whether shifts in the structure  
94 of covariation may underlie the movement of individual lineages into new ecological contexts.  
95 Nevertheless, they make it clear that environmental variation plays a major role in patterns of  
96 phenotypic integration. This body of work has clearly explained trait covariation in terms of plant  
97 ecology; we seek to address it in terms of plant evolution.

98

99 Here, we perform a novel analysis of macroevolutionary integration across Vitaceae (grapes and their  
100 relatives) to see whether evolvability in multivariate leaf phenotypes coincides with transitions across  
101 habitats. Our interests here follow two major themes: 1) identifying whether changes in covariation  
102 have the potential to explain major ecological shifts, and 2) reaching across the biological hierarchy to  
103 draw more explicit links between the apparently distinct levels of covariation and evolutionary process  
104 (microevolutionary, macroevolutionary, ecological) outlined above. We explored this by applying a  
105 novel phylogenetic approach to test for shifts in the structure of covariation in evolutionary divergences  
106 across a set quantitative leaf traits measured across Vitaceae, a clade that has undergone multiple  
107 transitions between temperate and tropical biomes. Previous work has found that major changes in leaf  
108 phenotype coincide with temperate-tropical transitions in *Viburnum* (Schmerler et al. 2012). We sought  
109 to ask whether these changes may themselves be facilitated by rearrangements of the structure of  
110 evolutionary covariation among leaf traits. As a final goal, we aimed to identify whether the population  
111 and quantitative genetic processes that give rise to patterns in the structure of covariation provide any  
112 explanatory power over macroevolutionary dynamics in phenotypic disparity and lineage  
113 diversification across clades.

114

### 115 **Methods and Materials**

116 *Data and code.* Leaf measurements across Vitaceae were obtained from Chen (2009). The following  
117 seven traits were included: leaf width, leaf length, petiole length, petiole width, distance between  
118 secondary veins, tooth location (distance from leaf base), and petiolule length (of lateral leaflets)  
119 These morphological data were cleaned and log-transformed prior to analysis. All data files and code  
120 used in the study are available at (WILL PROVIDE).

121

122 *Phylogeny.* We used the molecular phylogeny of Vitaceae published by Parins-Fukuchi (2018). We  
123 applied dates to this phylogeny by including the fossil lineages examined in the aforementioned study  
124 as node calibrations using treePL (Smith and O'Meara 2012). We did not include the fossils as tips in  
125 the dating and covariation analyses because they represent seeds and therefore would have been  
126 uninformative with regard to leaf trait covariation.

127

128 *Phylogenetic variation in evolutionary covariation.* We developed a novel approach to examine shifts  
129 in the structure of evolutionary covariation across a phylogeny. This approach builds conceptually upon  
130 the work of Parins-Fukuchi (2020b), by extending the basic framework to explore 1) how covarying  
131 evolutionary patterns between traits themselves shift along a phylogeny, and 2) by modeling the  
132 covariance structure more explicitly rather than simply relying on shared patterns in phenotypic  
133 disparity across traits.

134

135 We will start our explanation of the method using the simplest version of the model: one where the  
136 structure of covariation is shared across the entire phylogeny. We first perform an ancestral state  
137 reconstruction (ASR) under Brownian motion on each of the traits (Maddison 1991). From here, we  
138 estimate directional vectors of change along each branch by subtracting the value at each node from  
139 that of its parent. At this point, each trait has been transformed into a set of  $2n-2$  ( $n$  is the number of  
140 lineages included in the phylogeny) vectors of edgewise evolutionary divergence. We then construct a  
141 correlation matrix using the vectors for each trait. This measures the magnitude with which each trait  
142 pair undergoes coordinated evolutionary changes and the direction of the association (positive or  
143 negative). In other words, it gives the covariance between changes in population means. The precise  
144 evolutionary interpretation of this matrix, typically referred to as  $V$ , has been outlined by Felsenstein  
145 (1988) using the equation:

146

147  $V = GCG$  (eqn. 1)

148

149  $G$  is the genetic covariance matrix, while  $C$  represents the set of covariances in the selection vectors for  
 150 each pair of traits. Taken together,  $V$  is then defined sensibly through a combination of the set of  
 151 genetic constraints and the effects of coordinated selection regimes. As a side note, Felsenstein (1988)  
 152 gave an explicit philosophical critique of the method through which we construct  $V$ . Specifically, he  
 153 pointed out that ASRs are not true data, but instead inferences drawn from data. While we, of course,  
 154 agree on a philosophical level, we believe the method is sufficient for our aim of reconstructing broad  
 155 shifts in evolutionary covariation. Practically speaking, while ASRs are often rife with error, we  
 156 believe that our own questions can be adequately tackled with estimates containing relatively high  
 157 error. The most important aspect is identifying positive and negative correlations that particularly stand  
 158 out and how that structure changes across a tree. It is also worth noting that many phylogenetic  
 159 comparative methods have arisen since the time of Felsenstein's writing that use essentially the same  
 160 information we use here – traits mapped to a phylogeny – to derive robust historical inferences. We are  
 161 therefore confident in our approach given our purposes. Detailed examination of each pairwise trait  
 162 relationship, or a full breakdown and interpretation of the  $G$  and  $C$  components, may benefit from more  
 163 careful methodological consideration, or at least further validation that the resulting covariances are  
 164 numerically robust to this approach. However, such fine-scaled analysis is not included among our  
 165 goals at present.

166

167 Estimating  $V$  is fundamental to our approach. It provides a natural link between the population genetic  
 168 conceptualization of covariation and modularity, defined ultimately by  $G$ , and the patterns observed  
 169 over deeper timescales, including those explored by paleontologists and macroevolutionists. If we  
 170 observe shifts in  $V$ , we are forced to acknowledge the likely reality that those shifts are at least partially  
 171 facilitated by shifts in  $G$ . This is because we know, over shorter timescales, that selection tends to be  
 172 inhibited if it is misaligned with  $G$ . Of course, the reality is that  $C$  also likely shifts during major  
 173 ecological transitions. Any heterogeneity must therefore be considered as the sum of these population  
 174 processes.

175

176 To consider the possibility that the structure of modularity has shifted across the phylogeny, we defined  
 177 a heterogeneous model structured as a phylogenetic mixture of multivariate normal distributions. In the  
 178 single  $V$  model, we model  $V$  as a single multivariate normal distribution with a mean vector of expected  
 179 changes equal to zero (this is the expectation under Brownian motion) and covariance matrix equal to  
 180  $V$ . In order to more fairly compare  $V$  across the tree, we placed all traits on the same scale and rescaled  
 181 all estimated covariance matrices to correlation matrices. Examining covariance matrices instead may  
 182 also be a useful application of the method, by searching simultaneously for shifts in both evolutionary  
 183 rate and covariation patterns, but was not our goal here. The probability density function of this  
 184 distribution gives us a likelihood function with which to evaluate the evidence in favor of our model.  
 185 To find the best-supported set of covariance regimes, we employed an automated search algorithm  
 186 based on that implemented by Smith et al. (2022). A summary of the algorithm follows.

187

188 *The search algorithm.* The algorithm requires a specified minimum size threshold, defined by the  
 189 number of tips, for clades to be considered. For example, if we specify 10, clades with 10 or more tips  
 190 will be considered as possible shift points. This greatly improves computational efficiency and also  
 191 helps protect against estimating poorly defined covariance matrices on very small clades. For every  
 192 clade that meets this size criterion, a covariance matrix is then estimated using *only* the edges  
 193 subtending the clade root. The algorithm then proceeds as follows: evaluate the likelihood of a  
 194 combined model, whereby the data are characterized using two multivariate normal distributions, one  
 195 encompassing the proposed shift and the other encompassing the rest of the taxa in the tree. Calculate

196 the Akaike information criterion (AIC) value using this combined likelihood. If the AIC indicates an  
 197 improvement in fit, save the estimated parameters and AIC scores; if not, discard them. Rank all of the  
 198 shifts according to their improvement in AIC over the base (single regime) model. Proceed through this  
 199 ranked list. Retain each model that, when combined with the previously retained models in the ranked  
 200 list, yields an AIC improvement over the base model. This procedure has the benefit of naturally  
 201 identifying the optimal shift point in the case where several adjacent nodes all represent possible shift  
 202 locations. The ranking ensures that the best-supported location will be added first; others will have to  
 203 add significantly to the explanatory power of the model if they are to be included as a nested shift.

204

205 *Environmental habit.* We constructed a dataset characterizing the environmental occupancy of each  
 206 lineage, as defined by freezing tolerance. First, we generated a dataset of spatial occurrences across  
 207 Vitaceae by gathering data from the Global Biodiversity Information Facility (GBIF–  
 208 <https://www.gbif.org/>). We then extracted climate data across these locales using the Bioclim dataset  
 209 (<https://www.worldclim.org/data/bioclim.html>). We defined any lineage as freezing tolerant for which  
 210 2.5% or more of occurrences across their sampled geographic range experience minimum temperatures  
 211 at or below zero degrees celsius during the coldest month of the year. We then performed a parsimony  
 212 analysis to map freezing tolerance to the phylogeny in order to compare the location of shifts in  
 213 covariation structure to those in the environment.

214

215 *Diversification rate analysis.* We estimated lineage-specific diversification rates using MiSSE (see  
 216 Vasconcelos et al. 2022a), a likelihood-based, hidden state only, state-speciation and extinction model  
 217 implemented in *hisse* (Beaulieu and O'Meara 2016). Within MiSSE there are 52 possible models to  
 218 evaluate, so we used the function *MiSSEGreedy()* to automate the process of fitting a large set of  
 219 MiSSE models. The function first runs a chunk of models, determines the “best” based on AIC, then it  
 220 continues on from that complexity until all models in a chunk of complex models are greater than 10  
 221  $\Delta$ AIC units than the current best model. In this way, we only evaluated a set of models that are  
 222 reasonably parameter-rich with respect to the data set. We culled the resulting model set to remove any  
 223 redundant model fits. For example, if the maximum likelihood estimates are the same for turnover rate  
 224 in regime *A* and the turnover in regime *B* in a turnover rate varying-only model, it is essentially the  
 225 same as including a single turnover rate model twice. This would lower the weight of other models as a  
 226 consequence. It is recommended in these situations to remove the more complex of the two from the set  
 227 (Burnham and Anderson 2003). For each model, we obtained the marginal reconstructions of the  
 228 specified hidden states for each node and tip in the tree. We then summarized results based on  
 229 diversification rates model-averaged across only the tips that survived to the present. For a given  
 230 model, the marginal probability of each rate regime is obtained for every tip, and the rates for each  
 231 regime are averaged together using the marginal probability as a weight: a weighted average of these  
 232 rates is then obtained across all models using Akaike weights.

233

234 We used a paired *t*-test to assess whether model-averaged diversification rates are different across the  
 235 different evolutionary covariation regimes. However, before conducting this analysis we first identified  
 236 all “cherries” in the tree, which are two tips that are sisters to each other and share the same branch  
 237 length to the direct ancestral node. Within MiSSE, all sister tips should theoretically inherit the exact  
 238 rate class probabilities, meaning they have identical tip rates. This could artificially inflate or reduce  
 239 any means within a given regime. Therefore, as a precaution, we removed, at random, one of the two  
 240 taxa represented in a cherry (see Vasconcelos et al. 2022a).

241

242

243

244

## 245 **Results and Discussion**

246 *The structure of leaf evolutionary integration and climate shifts.*

247 A close relationship between leaf form and climate has long been recognized (e.g., Givnish 1987;  
248 Spicer et al. 2021). This is reflected by the repeated, independent evolution of particular leaf syndromes  
249 and functional traits in similar climates—e.g., more rounded, toothed and lobed leaves in temperate  
250 environments (e.g., Schmerler et al. 2012). The widespread use of leaf physiognomy as basis for  
251 paleoclimatic inferences is a testament to the close link between leaf form and climate (e.g., Wolf  
252 1971), but this relationship is not without complications (Peppe et al. 2010). For example, leaf traits  
253 concentrated in particular biomes or climatic regimes might be, at least in part, a byproduct of select  
254 lineages being overrepresented in those areas (Hinojosa et al. 2010; Little et al. 2010). Leaf forms  
255 associated with particular climates might also, in some cases, have arisen before the climates  
256 themselves, suggesting that new climatic regimes can serve as a filter for preadapted forms (Ackerly  
257 2004). More generally, because leaves possess developmentally integrated suites of traits, it is  
258 unrealistic to expect individual traits to respond to climatic changes in simple, predictable ways.  
259 Examining changes in the structure of leaf trait integration across climatic shifts offers a basis for  
260 understanding the evolutionary underpinnings of environmental transitions, beyond the correlation of  
261 individual traits with different climatic variables.

262  
263 Given that different suites of traits are associated with megathermal (‘tropical’) vs. mesothermal  
264 (‘temperate’) climates (Wolfe 1995), we might generally expect the structure of leaf trait covariance to  
265 differ between these types of environments. We also might expect the strength of integration to control  
266 the extent to which lineages are able to readily shift between such environments, with more relaxed  
267 integration creating an opportunity for more frequent tropical-temperate shifts. Vitaceae represent an  
268 excellent system for exploring these problems because it has considerable taxonomic diversity in both  
269 tropical and temperate environments, as well as broad variation in leaf form with regard to leaf size,  
270 complexity (simple vs. compound), lobing, and tooth size, structure, and density. The dataset examined  
271 here captures different properties of leaf size and venation and tooth density, traits that have clear  
272 relationships with both temperature and precipitation levels (Spicer et al. 2021). Our results, detailed  
273 below, broadly show that integration regimes of leaf traits correspond closely with climate, with the  
274 strength of integration determining the ease with which lineages can evolutionarily shift into different  
275 environments.

276  
277 *Environmentally-linked shifts in evolutionary covariation.* Our approach uncovered evidence for three  
278 distinct evolutionary covariation regimes across Vitaceae leaf traits (Fig. 1). These regimes are largely  
279 congruent with broad patterns in climatic shifts (Fig. 2). In particular, regime 0 corresponds closely to  
280 the set of Vitaceae lineages that made the most significant transitions into freezing habitats (e.g., *Vitis*,  
281 *Parthenocissus*, etc). The clade encompassing *Cissus*, *Tetrastigma*, and related lineages corresponds to  
282 another co-variational regime. *Ampelocissus* also occupies its own regime, perhaps delimiting a  
283 phenotypic shift that occurred during the movement of this genus back into tropical biomes. Although  
284 we reconstructed the ancestor of Vitaceae, and many early branches in the phylogeny, to be freezing-  
285 tolerant, this is perhaps at odds with the prevailing climate during the early diversification of family,  
286 ca. 70 to 45 mya. During this time, global temperatures were considerably warmer than the present, and  
287 freezing conditions were perhaps only present (if at all) at high elevations or high latitudes, at least  
288 until the onset of climatic deterioration in the mid to late Eocene (Zachos et al. 2001). Most Cretaceous  
289 to early Cenozoic Vitaceae fossils are known from middle to low latitudes (e.g., Chen and Manchester  
290 2007; Manchester et al. 2013), suggesting that the ancestors of most major lineages likely did not  
291 experience freezing conditions. However, early representatives of Vitaceae (or particular lineages) may  
292 have possessed traits (e.g., deciduousness) that predisposed them to thrive in freezing conditions.  
293 Furthermore, an accurate reconstruction of the climate occupancy of ancestral Vitaceae, although

294 certainly of interest, is not of central importance for the focal questions of this study. The critical  
295 finding is that major covariation regimes largely coincide with lineages occupying particular climatic  
296 conditions ('tropical' vs 'temperate'), suggesting that evolutionary shifts in leaf trait integration also  
297 coincide with (or underlie) major environmental shifts in Vitaceae.

298  
299 *Habitat shifts and covariation strength.* More climatically variable lineages had weaker integration, on  
300 average (Table 1). The lineages under regime 1, which encompasses both tropical and temperate  
301 lineages, displayed the lowest overall correlation strengths. There are at least two possible explanations  
302 for this pattern: 1) the environmentally disparate lineages encompassed under regime 1 may be more  
303 evolutionarily flexible and morphologically diverse because of trait parcellation, or 2) lineages within  
304 regime 1 may undergo shifts in the structure of G (the genetic covariance matrix) during these repeated  
305 movements into frozen habitats. In the former scenario, G is relaxed across the entire regime, allowing  
306 lineages moving into freezing habitats to easily accommodate any resulting shifts in C (the selective  
307 covariance matrix). In the latter, G remodels itself during shifts into freezing climates, perhaps in  
308 response to shifts in C. In this case, the appearance of relaxed covariation would actually be driven by  
309 averaging across several, variable, covariance regimes left undetected due to lineage sampling. Either  
310 of these scenarios would be reflective of evolutionary flexibility in the structure of integration and so  
311 distinguishing between them is not important here. For our purposes, we are content to accept that the  
312 repeated shifts into freezing climates observed in regime 1 are linked with either a covariance structure  
313 that is more relaxed overall, facilitating a range of responses to selection, or more evolutionary labile,  
314 undergoing rapid change to accommodate the demands of new environments. Either case suggests that  
315 evolution of the macroevolutionary covariance structure (and by extension, its constituent parts, G and  
316 C) facilitated tolerance of unpredictable and distinct habitats, encountered either by migration into new  
317 areas, or in response to long-term climate changes occurring in situ. While we focused on temperate-  
318 tropical shifts here (with respect to freezing), we also note that the species included in regime 1 also  
319 occupy diverse habitats with respect to precipitation, including shifts into xeric environments in  
320 continental Africa, Madagascar, and parts of the Neotropics, which might similarly be influencing  
321 patterns of trait integration in this regime.

322  
323 Comparing the patterns shown by regimes 0 and 1 with that of regime 2 illustrates how ecological  
324 specialization can generate covariance patterns that are more conserved at the macroevolutionary level.  
325 Regime 2, which is overwhelmingly specialized in tropical climates, displays the phylogenetic  
326 covariance matrix with the strongest structure and the strongest evolutionary links between traits, on  
327 average. On the surface, this result may appear to be at odds with ecological work on trait covariation  
328 within communities along environmental stress gradients (Dwyer and Laughlin 2017). Ecological work  
329 has found that more stressful environments host plant communities with stronger covariation between  
330 functional traits. This is because environmental stressors induce functional constraints that  
331 disadvantage certain trait combinations. Lineages that display unfavorable trait combinations are  
332 filtered out of certain areas. In this case, trait covariation actually serves as a catalyst, rather than  
333 constraint, for some lineages to move into more challenging environments. Nevertheless, trade-offs  
334 imposed by competing environmental stressors appear to create slightly more complex dynamics in  
335 covariation patterns (Brown et al. 2022). Along similar lines, we suggest that increased tradeoffs  
336 induced by the flexible and sometimes unpredictable climates occupied by lineages in temperate and  
337 mixed temperate-tropical regions lead to a more generally volatile structure of evolutionary covariance.  
338 In addition, while some climates may filter out lineages based on trait covariation patterns over  
339 ecological scales, our work shows how lineages themselves can shift the structure of trait covariation  
340 and occupy new habitats over macroevolutionary timescales.

341

342 *Diversification rates across covariation regimes.* We grouped regimes 0 and 2 into a single  
 343 diversification regime and compared against rates within regime 1 to test the hypothesis that the  
 344 relaxed structure of evolutionary covariation and repeated independent movements from tropical into  
 345 temperate habitats may have led to distinct macroevolutionary dynamics. We found significant  
 346 differences in rates of speciation, extinction, net diversification, and turnover when comparing across  
 347 covariation regimes (Table 2). The strength of leaf integration across Vitaceae is linked with  
 348 diversification rates. More tightly integrated lineages (regimes 0 and 2) exhibit lower turnover and  
 349 higher net diversification rates than more weakly integrated lineages (regime 1). This correlation  
 350 between leaf integration strength and diversification rates also may be linked to differences in climate  
 351 niche evolution across each regime. The repeated climatic shifts observed in regime 1 correspond to  
 352 overall higher turnover, and marginally lower net diversification. More climatically stable regimes,  
 353 which are also more tightly integrated, turnover less and generally have a higher net increase in  
 354 diversity as a result.

355  
 356 *Leaf evolvability, climate shifts, and macroevolutionary dynamics.* The shifts in macroevolutionary  
 357 covariance between leaf traits are the consequence of both shifting structures of multivariate selection  
 358 and genetic constraints. While it was not possible here, given data limitations, to disentangle the  
 359 relative influence of each of these in shaping patterns emergent at the phylogenetic scale, the  
 360 coincidence of repeated movements between tropical and freezing environments with shifts in the  
 361 structure of trait covariation suggests that vitaceous leaves are generally evolvable in response to  
 362 environmental changes. This is reflected in overall trait disparity, with the most climatically labile  
 363 lineages occupying the largest spread of morphospace (Fig. 3). In contrast, the less climatically diverse  
 364 lineages, housed within regimes 0 and 2, display lower disparity overall and tighter mean integration  
 365 between traits.

366  
 367 The patterns displayed across regime 1, which has undergone repeated movements into freezing  
 368 habitats from a tropical ancestor, provides a compelling example. While the lineages contained in  
 369 regimes 0 and 2 are relatively uniform in climate tolerance, regime 1 has repeatedly made the difficult  
 370 transition from tropical to freezing. The covariation pattern in regime 1 indicates enhanced  
 371 evolutionary flexibility, i.e., evolvability, as indicated by weakened integration as compared to the  
 372 other regimes (Table 1). The multivariate vectors of selection on leaf traits likely shift during  
 373 movement into new climates. The ability for lineages to withstand repeated shifts into freezing habitats  
 374 suggests that  $G$  likely does not strongly constrain response of the population means to the new  
 375 directions imposed by selection in these new environments. If  $G$  did maintain long-term constraints  
 376 across these transitions, these migrant lineages, constrained within a maladaptive phenotypic space  
 377 relative to their new habitats, would likely go extinct because of a decreased efficacy navigating these  
 378 new habitats and competition from perhaps better-adapted species (Van Valen 1973). Although we  
 379 analyzed these patterns in light of only *abiotic* (environmental) factors, we assume that new  
 380 environments will also contain different biotic contexts. And regardless of the relative importance of  
 381 biotic and abiotic factors in driving these macroevolutionary patterns, as originally formulated, the Red  
 382 Queen accommodates both. We favor this interpretation given that the two likely work synchronously.  
 383 We therefore assume that the environmental shifts we identified, along with the corresponding shifts in  
 384 phenotype and development, may indicate changes in both abiotic and biotic factors.

385  
 386 We observed a pattern of high leaf evolvability across environmental transitions paired with elevated  
 387 turnover rates in lineages transitioning into derived habitats. Diversification rate variation has been  
 388 explained by many possible dynamics, for example, latitudinal correlates with energy input: “the Red  
 389 Queen runs faster when she is hot” (Brown 2014). Our analyses reflect a somewhat simpler dynamic  
 390 that unifies several levels of macroevolutionary patterns. The patterns in Vitaceae suggest that *the Red*



391 *Queen runs faster when she is uncomfortable* (see similar arguments in Stebbins 1974; Vasconcelos et  
 392 al. 2022b). Encountering new habitats due to migration and/or climate change results in the emergence  
 393 of a completely new set of biotic and abiotic conditions that may yield a variety of responses that are  
 394 intrinsic to each individual lineage. These responses may be rooted in developmental and genetic  
 395 constraints on phenotypes, population-level variation, and extinction dynamics. As a result, while  
 396 extinction tends to increase when lineages encounter new habitats, this is compensated for by increased  
 397 speciation among phenotypically flexible lineages. Highly evolvable lineages, and perhaps those  
 398 preadapted as well (as lianas such as Vitaceae might be for a variety of conditions), are better equipped  
 399 to keep up with these novel and likely challenging conditions by increasing their evolutionary pace. In  
 400 the case of Vitaceae, this results in a more flexible phenotypic covariance structure, wider phenotypic  
 401 disparity, and elevated turnover rates. Further research identifying the specific link between phenotypic  
 402 innovation, constraint, and speciation rates will help to further refine our understanding of how lineages  
 403 persist in the face of a shifting evolutionary landscape.

404

405 This second layer might explain results in vertebrates that conflict with latitudinal explanations for  
 406 diversification rate variation (Rabosky et al., 2018), which found “paradoxically” higher speciation  
 407 rates far from the tropics. These patterns may reflect a more extreme manifestation of the causes we  
 408 outline here. Movement to more extreme environments may, in some lineages, increase variation in  
 409 macroevolutionary parameters (lineage diversification, the origin of phenotypic novelties, etc) to a  
 410 level that overwhelms latitudinal patterns. For example, certain ecological conditions in temperate and  
 411 arctic regions may be so far from a lineage’s initial capability to accommodate them that it must  
 412 increase its macroevolutionary activity beyond that displayed at the tropics to outpace extinction. This  
 413 may manifest itself in higher turnover, faster and wider phenotypic disparification, and  
 414 macroevolutionary integration patterns that are structured more flexibly. The relative importance of  
 415 latitudinal vs intrinsic explanations likely varies across clades, environments, and epochs. Deeper  
 416 understanding of the level(s) at which selection operates and how intrinsic evolvability interacts with  
 417 movement into new ecological contexts will help to further disentangle the root causes of these  
 418 dynamics and disparity in pattern across studies and taxa.

419

420 It also seems worthwhile to note that the lineages within regime 1 do not cluster according to climate  
 421 niche in leaf morphospace (Fig. 3). This suggests that, during repeated transitions back into freezing  
 422 climates, each lineage tends to carve out a unique evolutionary path and ultimately approach similar  
 423 environmental challenges with different phenotypic solutions. Alternatively, it is possible that variation  
 424 in other climatic variables is causing these lineages to diffuse into different regions of morphospace.  
 425 Shifts into arid habitats, which became more widespread during the Neogene, might have influenced  
 426 leaf evolution and morphospace occupancy in various ways, independently or alongside shifts into  
 427 freezing conditions.

428

429 *Shifts in macroevolutionary integration as a scale-unifying construct.* Our results provide one  
 430 illustration of the potential for a hierarchically integrated view of biological modularity. The  
 431 formulation of our model provides a bridge between quantitative and population genetics,  
 432 macroevolutionary patterns in multivariate trait disparity and lineage diversification, and ecological  
 433 dynamics. The modularity that emerges from covariation patterns at each level may combine in  
 434 complex ways to yield the evolutionary behaviors observed at subsequently higher levels.  
 435 Macroevolutionary integration patterns provide a bridge between these scales and a route through  
 436 which to more carefully dissect how processes at each scale interact to form the patterns we observe  
 437 across the tree of life. More broadly, investigating shifts in macroevolutionary integration can generate  
 438 a more hierarchically cohesive understanding of phenotypic evolution. Examining shifts in integration  
 439 between evolutionary divergences affords the potential to link the cumulative effects of well-

440 characterized population processes over macroevolutionary time. This framework can be further  
 441 leveraged to explain how shifts in multivariate complexity mapped to macroevolutionary timescales  
 442 correspond to major ecological shifts, thereby making the initial steps in a new framework through  
 443 which to seek a truly cohesive and view of biological complexity across temporal, taxonomic, and  
 444 spatial scales.

445

#### 446 **Acknowledgements**

447 The authors would like to thank Iju Chen and Steven Manchester for generously sharing raw leaf  
 448 measurements from Vitaceae specimens. We also thank NJ Walker-Hale, JB Pease, SA Smith, and JG  
 449 Saulsbury for many fruitful conversations. TPF would like to thank M Ahmad-Gawel, DL Mahler, L  
 450 Rowe, and J Sztepanacz for many useful conversations that helped guide the course of this work. This  
 451 manuscript is based on a presentation given by TPF at the colloquium “Innovation and Novelty in the  
 452 Evolution of Plants” at Botany 2022 in Anchorage, AK, USA. The authors were supported by National  
 453 Science Foundation grants DEB-2217117 awarded to TPF and DEB-1916558 awarded to JMB.

454

455

#### 456 **Tables**

Covariation regime	Mean absolute correlation strength
Regime 0	0.42
Regime 1	0.24
Regime 2	0.47

457

458 *Table 1.* Mean correlation strength within each reconstructed regime, calculated as the mean of the  
 459 absolute value of the correlations present in the correlation matrix reconstructed for each regime.

460

461

Covariation regime	$\lambda$	$\mu$	Net diversification ( $\lambda - \mu$ )	Turnover ( $\lambda + \mu$ )
0 + 2	0.442	0.376	0.059	0.818
1	0.569	0.500	0.043	1.070

462

463 *Table 2.* Mean diversification rates across covariation regimes. Given the similarities in the strength of  
 464 the correlation, as well as issues related to power, we combined covariation Regimes 0 and 2 and  
 465 compared against Regime 1. In all cases the differences shown are significant based on a paired *t*-test.

466

467

468

469

470

471

472

473

474

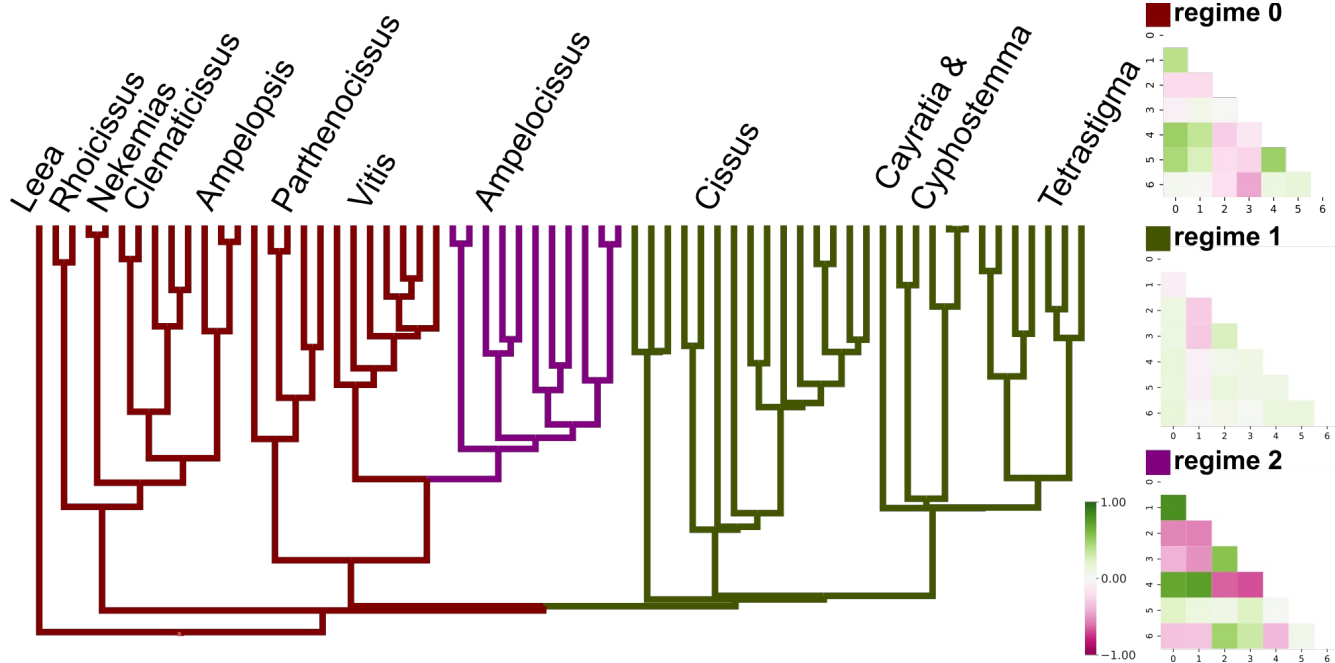
475

476

477

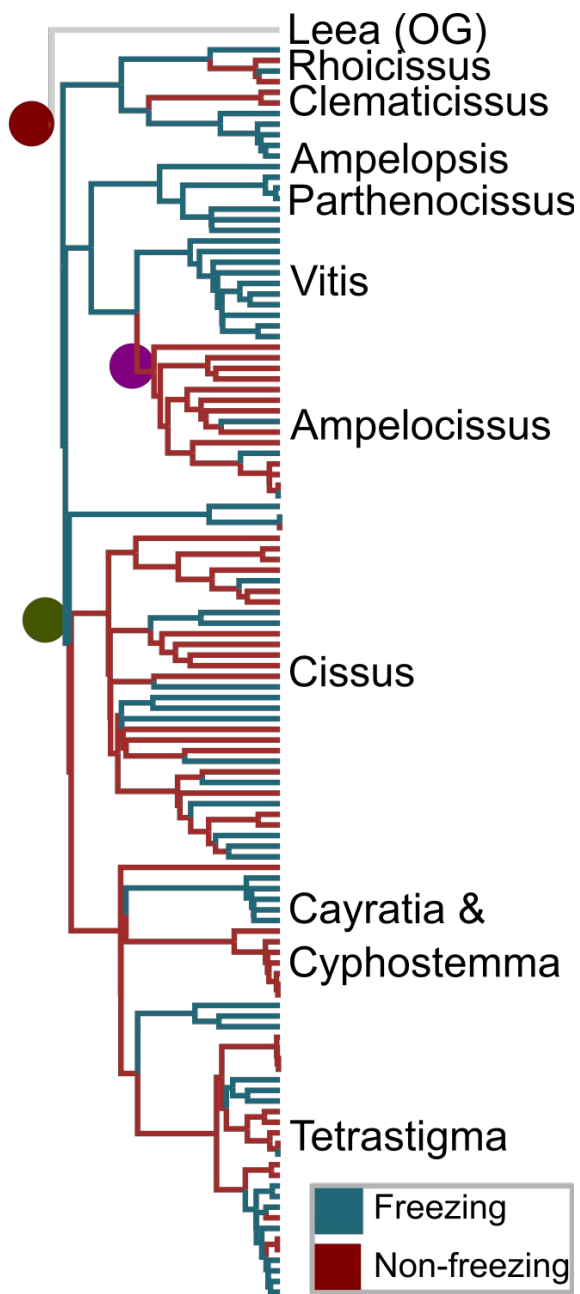
478  
479  
480  
481  
482  
483

## Figures



484  
485  
486  
487  
488  
489

*Figure 1.* Reconstructed macroevolutionary integration regimes mapped to Vitaceae phylogeny and reconstructions of covariation patterns displayed by each regime.



490

491

492 *Figure 2.* Freezing tolerance mapped to Vitaceae phylogeny. Coloured dots correspond to

493 macroevolutionary integration shift points. Reconstruction of climate tolerance was performed on a

494 superset of the taxa available for the morphological analyses. Taxa not included in the morphological

495 analyses were assumed to follow the same integration pattern as their nearest sibling taxa that were

496 present in the morphological analysis.

497

498

499

500

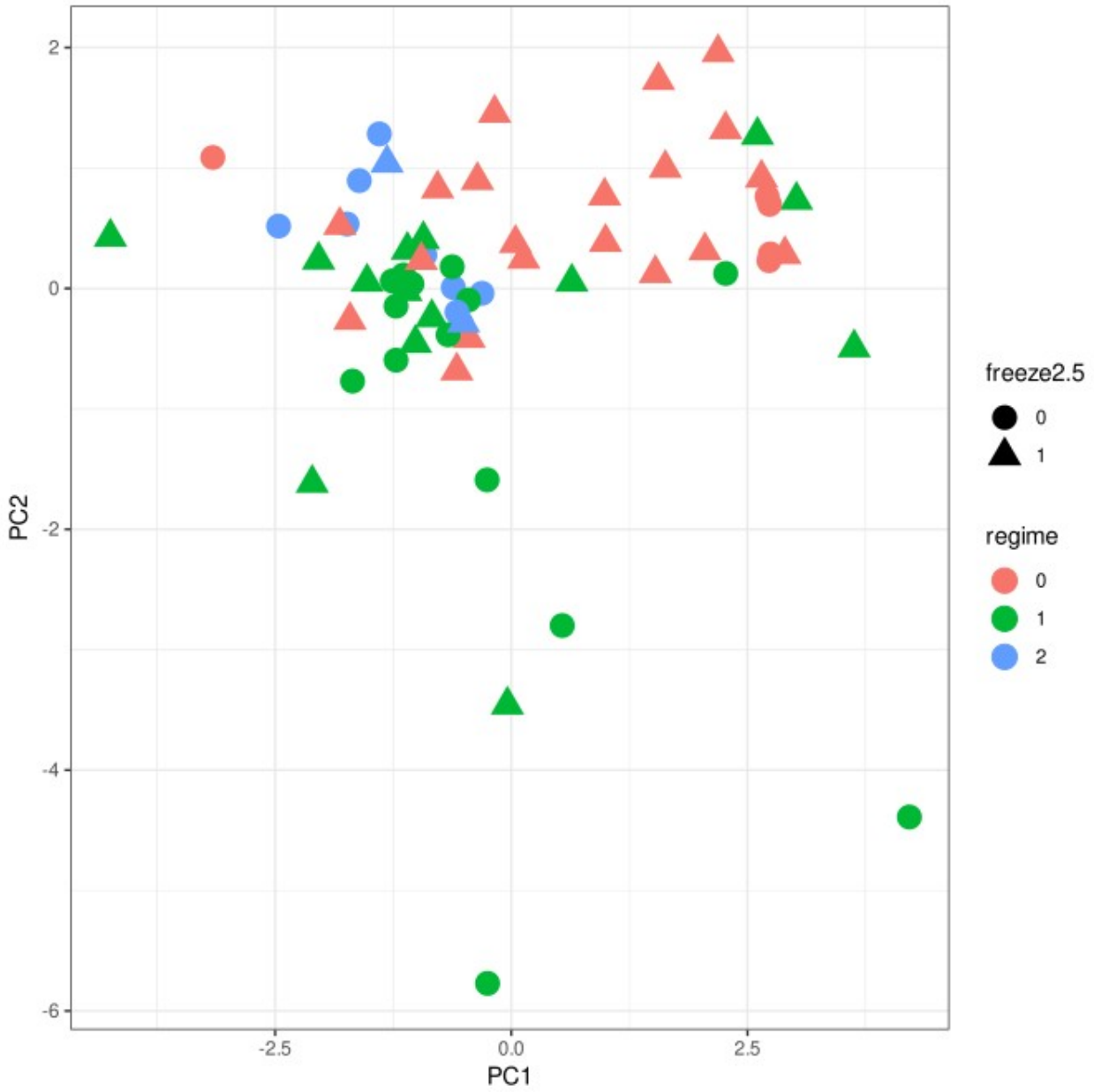
501

502

503

504

505  
506  
507  
508



509  
510  
511  
512  
513  
514  
515  
516  
517  
518  
519

Figure 3. Vitaceae leaf trait morphospace.

520 **References**

521

522 Ackerly DD, 2004. Adaptation, niche conservatism, and convergence: comparative studies of leaf  
523 evolution in the California chaparral. *The American Naturalist*, 163(5), 654-671.

524

525 Agrawal AF, Stinchcombe JR. 2009. How much do genetic covariances alter the rate of adaptation?  
526 *Proceedings of the Royal Society B: Biological Sciences*, 276(1659), 1183-1191.

527

528 Beldade P, Koops K, Brakefield PM. 2002. Developmental constraints versus flexibility in  
529 morphological evolution. *Nature*, 416(6883), 844-847.

530

531 Bolstad GH, Hansen TF, Pélabon C, Falahati-Anbaran M, Pérez-Barrales R, Armbruster WS. 2014.  
532 Genetic constraints predict evolutionary divergence in *Dalechampia* blossoms. *Philosophical*  
533 *Transactions of the Royal Society B: Biological Sciences*, 369(1649), p.20130255.

534

535 Brown A, Butler DW, Radford-Smith J, Dwyer JM. 2022. Changes in trait covariance along an  
536 orographic moisture gradient reveal the relative importance of light-and moisture-driven trade-offs in  
537 subtropical rainforest communities. *New Phytologist*.

538

539 Brown JH. 2014. Why are there so many species in the tropics?. *Journal of Biogeography*, 41(1), 8-22.

540

541 Chen I. 2009. History of Vitaceae Inferred from morphology-based phylogeny and the fossil record of  
542 seeds. PhD Dissertation, University of Florida.

543

544 Chen I, Manchester SR. 2007. Seed morphology of modern and fossil *Ampelocissus* (Vitaceae) and  
545 implications for phytogeography. *American Journal of Botany*, 94(9), 1534-1553.

546

547 Chenoweth SF, Rundle HD, Blows MW. 2010. The contribution of selection and genetic constraints to  
548 phenotypic divergence. *The American Naturalist*, 175(2), 186-196.

549

550 Cheverud JM. 1988. A comparison of genetic and phenotypic correlations. *Evolution*, 42(5), 958-968.

551

552 Cheverud JM. 1984. Quantitative genetics and developmental constraints on evolution by selection.  
553 *Journal of Theoretical Biology*, 110(2), 155-171.

554

555 Dwyer JM, Laughlin DC. 2017. Constraints on trait combinations explain climatic drivers of  
556 biodiversity: the importance of trait covariance in community assembly. *Ecology Letters*, 20(7), 872-  
557 882.

558

559 Felsenstein J. 1988. Phylogenies and quantitative characters. *Annual Review of Ecology and*  
560 *Systematics*, 445-471.

561

562 Goswami A, Binder WJ, Meachen J, O'Keefe FR. 2015. The fossil record of phenotypic integration  
563 and modularity: a deep-time perspective on developmental and evolutionary dynamics. *Proceedings of*  
564 *the National Academy of Sciences*, 112(16), 4891-4896.

565

566 Hansen TF, Pélabon C, Armbruster WS, Carlson ML. 2003. Evolvability and genetic constraint in  
567 *Dalechampia* blossoms: components of variance and measures of evolvability. *Journal of Evolutionary*  
568 *Biology*, 16(4), 754-766.

- 569  
570 Hansen TF, Houle D. 2008. Measuring and comparing evolvability and constraint in multivariate  
571 characters. *Journal of Evolutionary Biology*, 21(5), 1201-1219.  
572
- 573 Hinojosa LF, Pérez F, Gaxiola A, Sandoval I. 2011. Historical and phylogenetic constraints on the  
574 incidence of entire leaf margins: insights from a new South American model. *Global Ecology and*  
575 *Biogeography*, 20(3), 380-390.  
576
- 577 Houle D. 1992. Comparing evolvability and variability of quantitative traits. *Genetics*, 130(1), 195-204.  
578
- 579 Little SA, Kembel SW, Wilf P. 2010. Paleotemperature proxies from leaf fossils reinterpreted in light  
580 of evolutionary history. *PLoS One*, 5(12), p.e15161.  
581
- 582 Maddison WP. 1991. Squared-change parsimony reconstructions of ancestral states for continuous-  
583 valued characters on a phylogenetic tree. *Systematic Biology*, 40(3), 304-314.  
584
- 585 Manchester SR, Kapgate DK, Wen J. 2013. Oldest fruits of the grape family (Vitaceae) from the Late  
586 Cretaceous Deccan Cherts of India. *American Journal of Botany*, 100(9), 1849-1859.  
587
- 588 Melo D, Porto A, Cheverud JM, Marroig G. 2016. Modularity: genes, development and evolution.  
589 *Annual Review of Ecology, Evolution, and Systematics*, 47, 463.  
590
- 591 Melo D, Marroig G. 2015. Directional selection can drive the evolution of modularity in complex traits.  
592 *Proceedings of the National Academy of Sciences*, 112(2), 470-475.  
593
- 594 Parins-Fukuchi CT. 2018. Bayesian placement of fossils on phylogenies using quantitative  
595 morphometric data. *Evolution*, 72(9), 1801-1814.  
596
- 597 Parins-Fukuchi CT. 2020. Mosaic evolution, preadaptation, and the evolution of evolvability in apes.  
598 *Evolution*, 74(2), 297-310.  
599
- 600 Parins-Fukuchi CT. 2020. Detecting mosaic patterns in macroevolutionary disparity. *The American*  
601 *Naturalist*, 195(2), 129-144.  
602
- 603 Peppe DJ, Royer DL, Cariglino B, Oliver SY, Newman S, Leight E, Enikolopov G, Fernandez-Burgos  
604 M, Herrera F, Adams JM, Correa E. 2011. Sensitivity of leaf size and shape to climate: global patterns  
605 and paleoclimatic applications. *New Phytologist*, 190(3), 724-739.  
606
- 607 Rabosky DL, Chang J, Cowman PF, Sallan L, Friedman M, Kaschner K, Garilao C, Near TJ, Coll M,  
608 Alfaro ME, 2018. An inverse latitudinal gradient in speciation rate for marine fishes. *Nature*,  
609 559(7714), 392-395.  
610
- 611 Revell LJ, Collar DC. (2009). Phylogenetic analysis of the evolutionary correlation using likelihood.  
612 *Evolution*, 63(4):1090–1100.  
613
- 614 Revell LJ, Toyama KS, Mahler DL. 2022. A simple hierarchical model for heterogeneity in the  
615 evolutionary correlation on a phylogenetic tree. *PeerJ*, 10, p.e13910.  
616

- 617 Schmerler SB, Clement WL, Beaulieu JM, Chatelet DS, Sack L, Donoghue MJ, Edwards EJ. 2012.  
618 Evolution of leaf form correlates with tropical–temperate transitions in *Viburnum* (Adoxaceae).  
619 *Proceedings of the Royal Society B: Biological Sciences*, 279(1744), 3905-3913.  
620
- 621 Smith SA, O’Meara BC. 2012. treePL: divergence time estimation using penalized likelihood for large  
622 phylogenies. *Bioinformatics*, 28(20), 2689-2690.  
623
- 624 Smith SA, Walker-Hale N, Parins-Fukuchi CT. 2022. Compositional shifts associated with major  
625 evolutionary transitions in plants. *bioRxiv*.  
626
- 627 Spicer RA, Yang J, Spicer TE, Farnsworth A. 2021. Woody dicot leaf traits as a palaeoclimate proxy:  
628 100 years of development and application. *Palaeogeography, Palaeoclimatology, Palaeoecology*, 562,  
629 110138.  
630
- 631 Spriggs EL, Schmerler SB, Edwards EJ, Donoghue MJ. 2018. Leaf form evolution in *Viburnum*  
632 parallels variation within individual plants. *The American Naturalist*, 191(2), 235-249.  
633
- 634 Stebbins GL. 1974. *Flowering Plants: Evolution Above the Species Level*. Harvard University Press.  
635 Cambridge, MA, USA. 9780674864856.  
636
- 637 Swenson NG. 2014. Phylogenetic imputation of plant functional trait databases. *Ecography*, 37(2), 105-  
638 110.  
639
- 640 Sztepanacz JL and Houle D. 2019. Cross-sex genetic covariances limit the evolvability of wing-shape  
641 within and among species of *Drosophila*. *Evolution*, 73(8), 1617-1633.  
642
- 643 Wagner GP, Altenberg L. 1996. Complex adaptations and the evolution of evolvability. *Evolution*,  
644 50(3).  
645
- 646 Wagner GP, Pavlicev M, Cheverud JM. 2007. The road to modularity. *Nature Reviews Genetics*, 8(12),  
647 921-931.  
648
- 649 Wagner PJ, 2018. Early bursts of disparity and the reorganization of character integration. *Proceedings*  
650 *of the Royal Society B*, 285(1891), 20181604.  
651
- 652 Wolfe JA. 1971. Tertiary climatic fluctuations and methods of analysis of Tertiary floras.  
653 *Palaeogeography, Palaeoclimatology, Palaeoecology*, 9(1), 27-57.  
654
- 655 Wolfe JA. 1995. Paleoclimatic estimates from Tertiary leaf assemblages. *Annual Review of Earth and*  
656 *Planetary Sciences*, 23, 119-142.  
657
- 658 Van Valen L. 1973. A new evolutionary law. *Evolutionary Theory*, 1(1), 1-30.  
659
- 660 Vasconcelos T, O’Meara BC, Beaulieu JM. 2022a. A flexible method for estimating tip diversification  
661 rates across a range of speciation and extinction scenarios. *Evolution* 76: 1420-1433.  
662
- 663 Vasconcelos T, O’Meara BC, Beaulieu, JM. 2022b. Retiring "cradles" and "museums" of biodiversity.  
664 *American Naturalist* 199: 194-205.  
665



- 666 Vermeij GJ, 1973. Adaptation, versatility, and evolution. *Systematic Zoology*, 22(4), 466-477.  
667
- 668 Zachos J, Pagani M, Sloan L, Thomas E, Billups K. 2001. Trends, rhythms, and aberrations in global  
669 climate 65 Ma to present. *science*, 292(5517), 686-693.  
670  
671  
672  
673  
674  
675  
676  
677  
678  
679  
680  
681  
682